Anal Bioanal Chem (2011) 401:2995–3009
DOI 10.1007/s00216-011-5370-z

ORIGINAL PAPER

Feasibility of using atmospheric pressure matrix-assisted laser desorption/ionization with ion trap mass spectrometry in the analysis of acetylated xylooligosaccharides derived from hardwoods and *Arabidopsis thaliana*

Sun-Li Chong · Teemu Nissilä · Raimo A. Ketola · Sanna Koutaniemi · Marta Derba-Maceluch · Ewa J. Mellerowicz · Maija Tenkanen · Päivi Tuomainen

Received: 9 June 2011 / Revised: 23 August 2011 / Accepted: 25 August 2011 / Published online: 9 September 2011

Abstract The atmospheric pressure matrix-assisted laser desorption/ionization with ion trap mass spectrometry (AP-MALDI-ITMS) was investigated for its ability to analyse plant-derived oligosaccharides. The AP-MALDI-ITMS was able to detect xylooligosaccharides (XOS) with chain length of up to ten xylopyranosyl residues. Though the conventional MALDI–time-of-flight/mass spectrometry (TOF/MS) showed better sensitivity at higher mass range (>*m/z* 2,000), the AP-MALDI-ITMS seems to be more suitable for detection of acetylated XOS, and the measurement also corresponded better than the MALDI-TOF/MS analysis to the actual compositions of the pentose- and hexose-derived oligosaccharides in a complex sample. The structures of two isomeric aldotetrauronic acids and a mixture of acidic XOS were elucidated by AP-MALDI-ITMS using multi-stages mass fragmentation up to MS^3. Thus, the AP-MALDI-ITMS demonstrated an advantage in determining both mass and structures of plant-derived oligosaccharides. In addition, the method of combining the direct endo-1,4-β-D-xylanase hydrolysis of plant material, and then followed by AP-MALDI-ITMS detection, was shown to recognize the substitution variations of glucuronoxylans in hardwood species and in *Arabidopsis thaliana*. To our knowledge, this is the first report to demonstrate the acetylation of glucuronoxylan in *A. thaliana*. The method, which requires only a small amount of plant material, such as 1 to 5 mg for the *A. thaliana* stem material, can be applied as a high throughput fingerprinting tool for the fast comparison of glucuronoxylan structures among plant species or transformants that result from in vivo cell wall modification.

Keywords Acetylation · 4-*O*-Methylglucuronoxylan · Endo-1,4-β-D-xylanase · AP-MALDI mass spectrometry · Hardwood · *Arabidopsis thaliana*

Electronic supplementary material The online version of this article (doi:10.1007/s00216-011-5370-z) contains supplementary material, which is available to authorized users.

S.-L. Chong (✉) · S. Koutaniemi · M. Tenkanen · P. Tuomainen
Department of Food and Environmental Sciences,
Faculty of Agriculture and Forestry, University of Helsinki,
P.O. Box 27, 00014 Helsinki, Finland
e-mail: sun-li.chong@helsinki.fi

T. Nissilä · R. A. Ketola
Centre for Drug Research, Faculty of Pharmacy,
University of Helsinki,
P.O. Box 56, 00014 Helsinki, Finland

T. Nissilä · R. A. Ketola
Division of Pharmaceutical Chemistry, Faculty of Pharmacy,
University of Helsinki,
P.O. Box 56, 00014 Helsinki, Finland

M. Derba-Maceluch · E. J. Mellerowicz
Umeå Plant Science Centre, Department of Forest Genetics and Plant Physiology, Swedish University of Agricultural Sciences,
901-83 Umeå, Sweden

Introduction

Xylans are the most abundant hemicelluloses present in the cell walls of monocots and dicots. Their structures are heterogenic, and their compositions vary depending on the plant origin [1]. The glucuronoxylans (GX) in dicots, such as hardwoods, consist of linear (1→4)-linked β-D-xylopyranosyl residues as backbone, which is randomly substituted by (1→2)-linked 4-*O*-methyl-α-D-glucopyranosyl uronic

acid (meGlcA) and/or α-D-glucopyranosyl uronic acid (GlcA) [1–3]. In addition, GX contain a high number of acetyl groups esterified at O3 and/or O2 xylopyranosyl residues [3–6]. The biosynthesis studies of GX are important for the understanding about its function in plant growth and for the better utilization of biomass in biotechnological application. It is presently almost solely carried out with *Arabidopsis thaliana*, a model dicot plant whose genome has been sequenced [7–9].

GX are commonly isolated from the cell wall material by alkaline solutions. However, ester bonds are readily saponified in alkaline conditions, thus resulting in the deacetylation of GX [10]. For detailed structural studies, information on the intact xylans is needed in order to gain complete structural information on the native plant cell wall components. One possible method is to apply specific enzymatic hydrolysis to liberate directly the selected oligosaccharides from the plant cell wall, followed by detection through sensitive analytical systems, such as mass spectrometry (MS) [11, 12]. The direct enzymatic hydrolysis of plant materials reduces the risks for structural modifications due to chemical treatments. The method developed by Lerouxel et al. [11] used xyloglucan specific endoglucanase to liberate xyloglucan oligosaccharides from the *A. thaliana* mutants, in combination with matrix-assisted laser desorption/ionization–time-of-flight/MS (MALDI-TOF/MS) detection to elucidate the differences of xyloglucan structures among mutants. Recently, Westphal et al. [12] devised an enzyme cocktail, which contains multiple polysaccharide (cellulose, pectin, xylan and xyloglucan) degrading enzymes, to liberate several types of plant cell wall-derived oligosaccharides that were detected by using a MALDI-TOF/MS system to identify further the changes in the corresponding polysaccharides present in the plant cell wall.

MS is a powerful tool used to analyse oligosaccharides. It provides faster speed of analysis and has the ability to analyse a significantly lower amount of sample, at least in comparison with the nuclear magnetic resonance (NMR) spectroscopy [13]. The MALDI-TOF/MS system is able to ionize underivatised oligosaccharides and determine the mass of analyte ions over a wide mass range. Therefore, this system is widely used to identify the masses of various oligosaccharides that are derived from different plant cell wall polysaccharides, such as cellulose [14], glucuronoxylan [4, 15, 16], glucomannan [17], (galacto)glucomannan [18] and pectin [19]. The vacuum MALDI ion source was, however, found to impart higher internal energy to the ions and caused more metastable fragmentation relative to ambient ionization [20]. The cleavages of labile sialic acid from sialylated carbohydrates were commonly observed upon ionization with the vacuum MALDI, and therefore, derivatization of the sialylated carbohydrates [21] was needed to maintain the sialic acid residues on the oligosaccharides moieties.

The ionization of oligosaccharides at atmospheric pressure using electrospray ionization (ESI) has also become increasingly important. A recent report showed the analysis of per-*O*-methylated xylotriose using atmospheric pressure photoionization MS (APPI/MS) [22]. The ESI combined with ion trap (IT) MS has been shown as a powerful tool to identify structures of oligosaccharides, such as per-*O*-methylated isomeric xylooligosaccharides (XOS) [23, 24] or underivatised oligosaccharides derived from glucuronoxylan [25, 26] and arabinoxylan [27], due to the advantage of the ITMS to perform multi-stages mass fragmentation in positive or negative ion mode. However, the ESI system showed to have lower sensitivity than MALDI, and derivatization of the oligosaccharides were sometimes required to enhance the sensitivity of the measurement [28]. The analyte signals in ESI can also be distributed among singly and multiply charged ions, and thus, the sensitivity of analyte signals can be reduced. MALDI produces predominantly sodium adducts analytes $[M+Na]^+$ from underivatised oligosaccharides [29].

Atmospheric pressure MALDI (AP-MALDI), incorporated with an orthogonal acceleration TOF (oaTOF), was developed by Laiko et al. [30] to analyse mixtures of peptides. The analysis of oligosaccharides has also been performed by combining the AP-MALDI ion source with other mass analysers, such as ITMS [31] and Fourier transform ion cyclotron resonance (FTICR) MS [32]. These studies showed that the ionization of analytes in AP-MALDI was softer than in the vacuum MALDI due to collision interaction with surrounding gas, and thus, the internal energy within the analyte ions was reduced. Therefore, the AP-MALDI was able to reduce the metastable fragmentation of labile oligosaccharides and was suitable to analyse carbohydrates containing labile groups such as sialic acid, sulphate and fucosyl residues [30–34]. In addition, the AP-MALDI combined with ITMS showed potential to perform multiple stages fragmentation (MS^n) to obtain linkage and branching information on the N-linked glycans [31]. However, there are no reports that describe the analysis of plant-derived oligosaccharides using AP-MALDI.

In this work, we evaluate the potential of AP-MALDI-ITMS in the analysis of plant cell wall-derived acetylated XOS and compare that with the performance of the vacuum MALDI-TOF. Further, the acetylated XOS, liberated by the direct hydrolysis of the cell wall preparations from the wood of three hardwood species (aspen, birch and eucalyptus) and from stems of *A. thaliana* with a glycoside hydrolase (GH) family 10 endo-1,4-β-D-xylanase, were analysed with AP-MALDI-ITMS for the GX structural comparison. The potential of AP-MALDI-ITMS to perform structural elucidation of aldouronic acid isomers and a

mixture of acidic XOS that resulted from the GH10 endo-1,4-β-D-xylanase hydrolysis of deacetylated hybrid aspen wood preparation is also demonstrated.

Materials and methods

Chemicals, carbohydrates and enzymes

Anhydrous sodium acetate, 2,5-dihydroxybenzoic acid (DHB), trifluoroacetic acid (TFA) and ammonium sulphate ($(NH_4)_2SO_4$) were obtained from Merck (Darmstadt, Germany). Sodium hydroxide (NaOH) was obtained from J.T. Baker (Avantor Performance Materials, Phillipsburg, NJ, USA). HPLC grade acetonitrile (ACN) was obtained from Labscan (Dublin, Ireland). MilliQ water (Millipore, Billerica, MA, USA) was used to prepare all of the solutions. The acetylated XOS sample isolated from hydrothermally treated *Eucalyptus globulus* wood [35] was a kind gift from Prof. Juan Carlos Parajó of the University of Vigo, Spain. The analytical methods used for the composition analysis were as described by Gullón et al. [35]. Pure endo-1,4-β-D-xylanase of *Aspergillus aculeatus* from the glycoside hydrolase family 10 (GH10) was a kind gift from Novozymes A/S (Bagsvaerd, Denmark).

Sample preparations

The ground wood powders from three hardwood species (aspen, birch and eucalyptus) were kind gifts from Prof. Stefan Willför of the Åbo Akademi University, Finland. The ground wood of young hybrid aspen (*Populus tremula* L.× *tremuloides* Michx.) was obtained from trees grown in the greenhouse at the Umeå Plant Science Center, Sweden. The alcohol insoluble residues (AIR) of aspen, birch, eucalyptus and hybrid aspen were prepared by boiling the wood powders in absolute ethanol (EtOH) twice, followed by washing twice in 50% EtOH. The ethanol solution was aspirated after centrifugation, and the residues were freeze-dried. Thirty milligrams of hybrid aspen AIR was further deacetylated by incubation in 50 mM NaOH (pH 12.7) at room temperature for 24 h. The residue was washed twice in MilliQ water followed by a wash with a 50-mM sodium acetate buffer (pH 5.0).

The *A. thaliana* ecotype Colombia plants were grown at 22 °C for a 16-h photoperiod until maturity (approximately 8 weeks). Ten-centimetre segments of basal inflorescence stems were frozen in liquid nitrogen and freeze-dried. The material was ground in a ball mill (30 Hz, 90 s), transferred to 80% EtOH in 4 mM 4-(2-hydroxyethyl)-1-piperazineethanesulfonic acid (HEPES) and incubated in 80 °C for 30 min. It was then centrifuged, and the pellet was washed successively with 70% EtOH, methanol:chloroform (1:1, *v/v*) and acetone. Finally, the pellet was dried overnight in a vacuum desiccator. The starch was removed through a procedure described by Zablackis et al. [36], using α-amylase (Sigma A6380), 835 nkat (50 U) per 10 mg of dry pellet material dissolved in 1 ml of 0.1 M potassium phosphate buffer at pH 7.0. The samples were incubated at 30 °C for 24 h, two times, and the pellet was washed with the buffer, then with water and twice with acetone. De-starched AIR was dried overnight in a vacuum desiccator.

The AIR derived from hardwood (aspen, birch and eucalyptus), deacetylated hybrid aspen wood and *A. thaliana* stems were incubated in a 20-mM sodium acetate buffer (pH 5.0), with the GH10 endo-1,4-β-D-xylanase of *A. aculeatus* (15,000 nkat/g AIR), for 24 h. The concentrations for hardwoods and *A. thaliana* were 15 and 5 mg AIR/ml, respectively.

Sample pre-treatment prior to MS measurement

The XOS samples, which were isolated from hydrothermally treated *E. globulus* wood and GH10 endo-1,4-β-D-xylanase hydrolysates of hardwoods and *A. thaliana*, were desalted and separated into neutral and acidic XOS using Hypersep Hypercarb Porous Graphitized Carbon (PGC) columns (Thermo Scientific, Waltham, MA, USA), according to the established protocols [37]. The neutral and acidic XOS were eluted from the column by 50% (*v/v*) ACN and 50% (*v/v*) ACN in 0.05% (*v/v*) TFA, respectively. Eluted XOS fractions were dried and dissolved in 10 to 50 μl of MiliQ water.

AP-MALDI-ITMS and MALDI-TOF/MS instrumentations

The DHB solution (10 mg/ml) was employed as matrix for both AP-MALDI-ITMS and MALDI-TOF/MS. The 10-mg DHB was dissolved in 1 ml ACN/MilliQ water (3:7, *v/v*). The neutral oligosaccharides were crystallized on a target plate by mixing 1 μl of the sample with 1 μl of the DHB solution, followed by drying under a constant stream of warm air. The acidic oligosaccharides sample were pre-mixed with DHB and $(NH_4)_2SO_4$ (7 mg/ml) solutions according to procedures described by Enebro et al. [38]. A 5-μl acidic oligosaccharides sample was added into an Eppendorf tube that contained a 20-μl DHB solution; after which, a 0.5-μl $(NH_4)_2SO_4$ solution was added. A 1-μl mixture solution was crystallized on a target plate, followed by drying under a constant stream of warm air.

The AP-MALDI-ITMS was the combination of an AP-MALDI ion source (Mass Tech Inc., Columbia, MD, USA) and Agilent 6330 ion trap mass spectrometer (Agilent Technologies, Waldbronn, Germany). The AP-MALDI ion source was operated as described by Salo et al. [39], with some modifications. The extended capillary was operated

with a potential of 3,200 V to direct ions formed at the ion trap; the drying gas was set to a flow rate of 5 L/min and temperature of 300 °C. The ion trap settings were as follows: the accumulation time was 100 ms, the "averages" were set at 10 and the "rolling averaging" was "on". The voltages of the skimmer and capillary exit were 40 and −200 V, respectively. The detection mass range was set from *m/z*300 to 2,000, and the ultra scan mode was chosen. For MS/MS measurements, the cut-off value was set to 30%, and the fragmentation amplitude were set from 0.7 to 0.9 V. The ion trap MS was calibrated by using the ESI tuning mix that was provided by the instrument manufacturer (Agilent Technologies, Waldbronn, Germany).

The MALDI-TOF Ultraflex system (Bruker Daltonics, Bremen, Germany) was equipped with a 337-nm laser, and the mass spectra were acquired in a positive ion mode. The operating parameters were as follows: acceleration voltage of 25 kV, delay extraction time of 40 ns and the ions were detected in a reflector mode. The TOF mass spectrometer was calibrated by commercial peptide standards (Bruker Daltonics, Bremen, Germany).

Calculation of percentage peak intensities

The peak intensities corresponding to meGlcA-XOS were extracted from the AP-MALDI-ITMS raw data for percentage intensities calculation. In the case of the eucalyptus samples, the peak intensities corresponding to the meGlcA-XOS carrying a hexose residue was summed together with the meGlcA-XOS in similar XOS chain length but without the hexose residue. The percentage peak intensity was calculated by dividing the intensity of a single peak with the total sum of the peak intensities in each acidic profile and then converted to a percentage value.

Preparation of isomeric aldotetrauronic acid for MS^n analysis

Two isomeric pure aldotetrauronic acid, 4-*O*-Me-α-D-Glc*p*A-(1→2)-β-D-Xyl*p*-(1→4)-β-D-Xyl*p*-(1→4)-β-D-Xyl*p* and β-D-Xyl*p*-(1→4)-[4-*O*-Me-α-D-Glc*p*A-(1→2)]-β-D-Xyl*p*-(1→4)-β-D-Xyl*p*, later named as UXX and XUX, respectively [40], were prepared by applying specific GH5, GH10 and GH11 endoxylanase hydrolysis, which was followed by chromatographic purification according to the protocols described by Koutaniemi et al. (in preparation).

Analysis of wood

The non-cellulosic polysaccharides in aspen, birch and eucalyptus wood powders were degraded by acid methanolysis, according to the method described by Sundberg et al. [41]. The methylated monosaccharides were further trimethylsilylated and analysed by gas chromatography (GC), according to the protocol described by Pastell et al. [42]. The monosaccharide standards used were D-xylose (Merck) and D-glucuronic acid sodium monohydrate (Aldrich). Quantification was performed using five concentration levels of each sugars, and D-sorbitol (Aldrich) was used as internal standard. The content of acetylation was determined by the incubation of the wood powders overnight in 0.1 M NaOH, followed by the analysis of the resulting acetic acid content with the Megazyme acetic acid assay kit (K-ACET; Bray, Ireland).

Results and discussion

Analysis of the XOS sample from *E. globulus* wood by AP-MALDI-ITMS and MALDI-TOF/MS

The feasibility of AP-MALDI-ITMS for the analysis of plant-derived oligosaccharides was first evaluated by analysing a mixture of acetylated XOS isolated from the hydrothermally treated *E. globulus* wood. The sample was separated into neutral and acidic XOS prior to MS measurement to ease the interpretation of mass spectra and to circumvent the problem of competition for ionization. Both neutral and acidic XOS were also analysed by MALDI-TOF/MS for comparison.

The mass spectra obtained from the measurement of the neutral XOS are shown in Fig. 1, and their corresponding annotated masses are listed in Electronic Supplementary Material Table S1a. A series of XOS that were substituted by acetyl groups was observed from both mass spectra as their sodium adducts ion peaks. The XOS chain lengths from two to nine xylopyranosyl residues with one to five acetyl residues were detected by both systems. Minor peaks representing non-acetylated xylobiose, xylotriose and xylotetraose were also detected. The main peaks that were observed from the AP-MALDI-ITMS mass spectrum were $Xyl_2(Ac_1)$, $Xyl_3(Ac_1)$, $Xyl_3(Ac_2)$ and $Xyl_4(Ac_2)$; from the MALDI-TOF mass spectrum, the main peaks were $Xyl_2(Ac_1)$, $Xyl_3(Ac_1)$ and $Xyl_4(Ac_2)$. The $Xyl_3(Ac_2)$ was less visible than the other three acetylated XOS in the MALDI-TOF/MS mass spectrum. In addition, there were peaks representing XOS with a higher degree of acetylation, $Xyl_3(Ac_3)$, $Xyl_4(Ac_4)$ and $Xyl_5(Ac_5)$, in each chain length series that were detected by the AP-MALDI-ITMS only.

A series of hexose oligosaccharide (HOS) peaks from two to seven residues were also detected (Electronic Supplementary Material Table S1b); however, the sensitivity of the measurement in the two systems was different. The MALDI-TOF/MS detected a significantly higher level

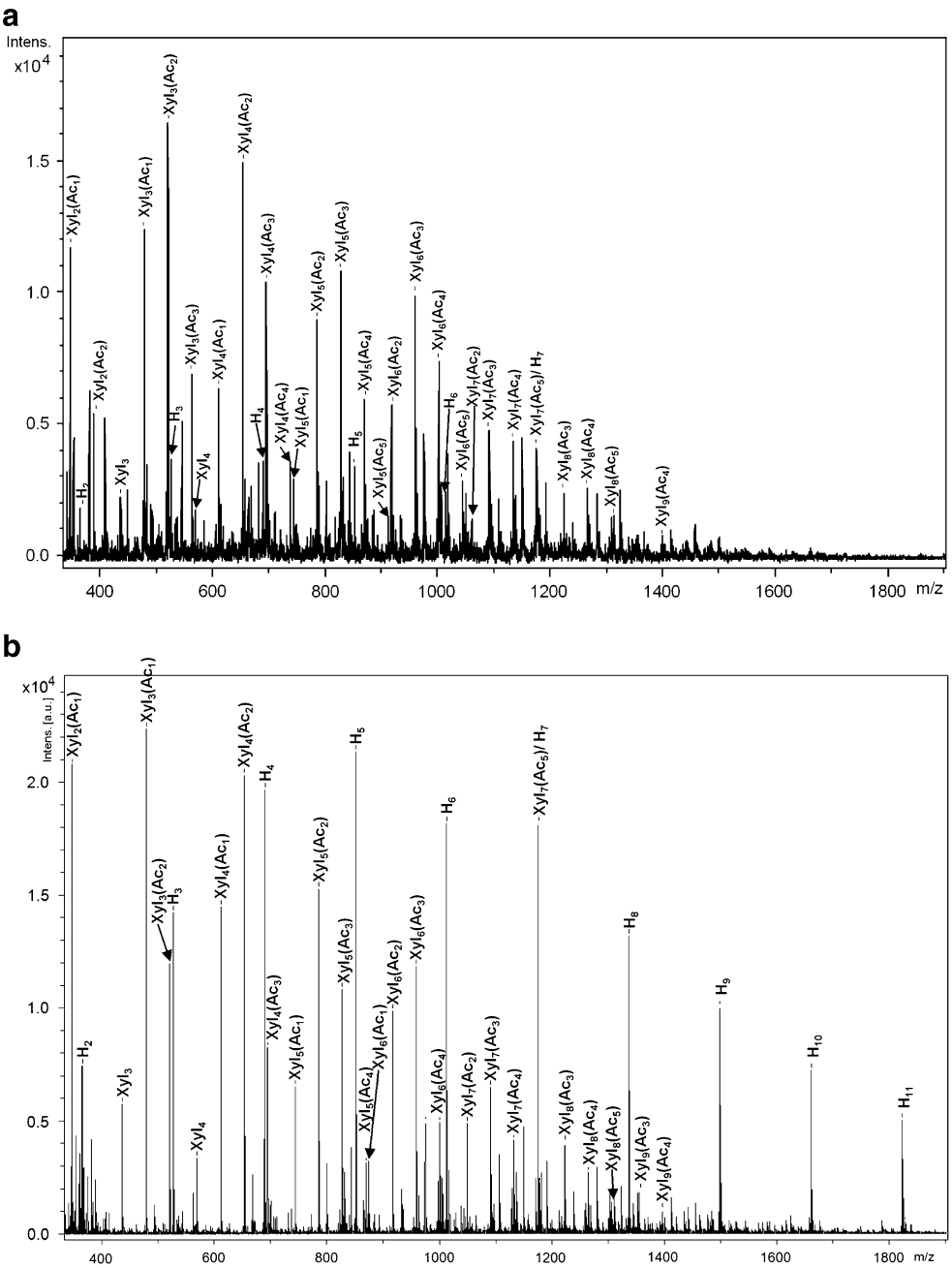

Fig. 1 A mass spectrum showing ion peaks (sodium adduct) representing neutral oligosaccharides purified from *Eucalyptus globulus* wood hydrolysate measured by (**a**) AP-MALDI-ITMS and (**b**) MALDI-TOF/MS

of HOS, especially for the longer HOS; the AP-MALDI-ITMS, on the other hand, detected only a low abundant HOS, compared to that of XOS, in the same mass spectra (Fig. 1a, b). The amount of anhydromonosaccharides and acetyl substituents in the XOS sample were 59% (*w/w*) xylose, 6.7% (*w/w*) uronic acid, 4% (*w/w*) hexoses and 14.5% (*w/w*) acetyl groups. The hexose content in the sample was approximately 15 times lower than the pentose content, indicating that the AP-MALDI-ITMS measurement represented the actual composition in this XOS sample better.

DHB has been the most used matrix in carbohydrate analysis with MALDI-TOF/MS [29]. However, the carboxylic groups present in the acidic oligosaccharides are prone to adduct formation; therefore, mono- and disodium adduct peaks are commonly observed when the mass spectra are acquired in the positive ion mode. The mass spectra have been simplified by the addition of $(NH_4)_2SO_4$ into the matrix sample mixture due to the affinity of the sulphate anion on alkali metals [43]. Due to the addition of $(NH_4)_2SO_4$, the ion peaks detected from the measurement of acidic oligosaccharides with AP-MALDI-ITMS and MALDI-TOF/MS were thus mostly mono-sodium adduct peaks (Fig. 2 and Electronic Supplementary Material Table S2). The acidic oligosaccharides were mainly a series of XOS carrying one meGlcA residue and substituted by a

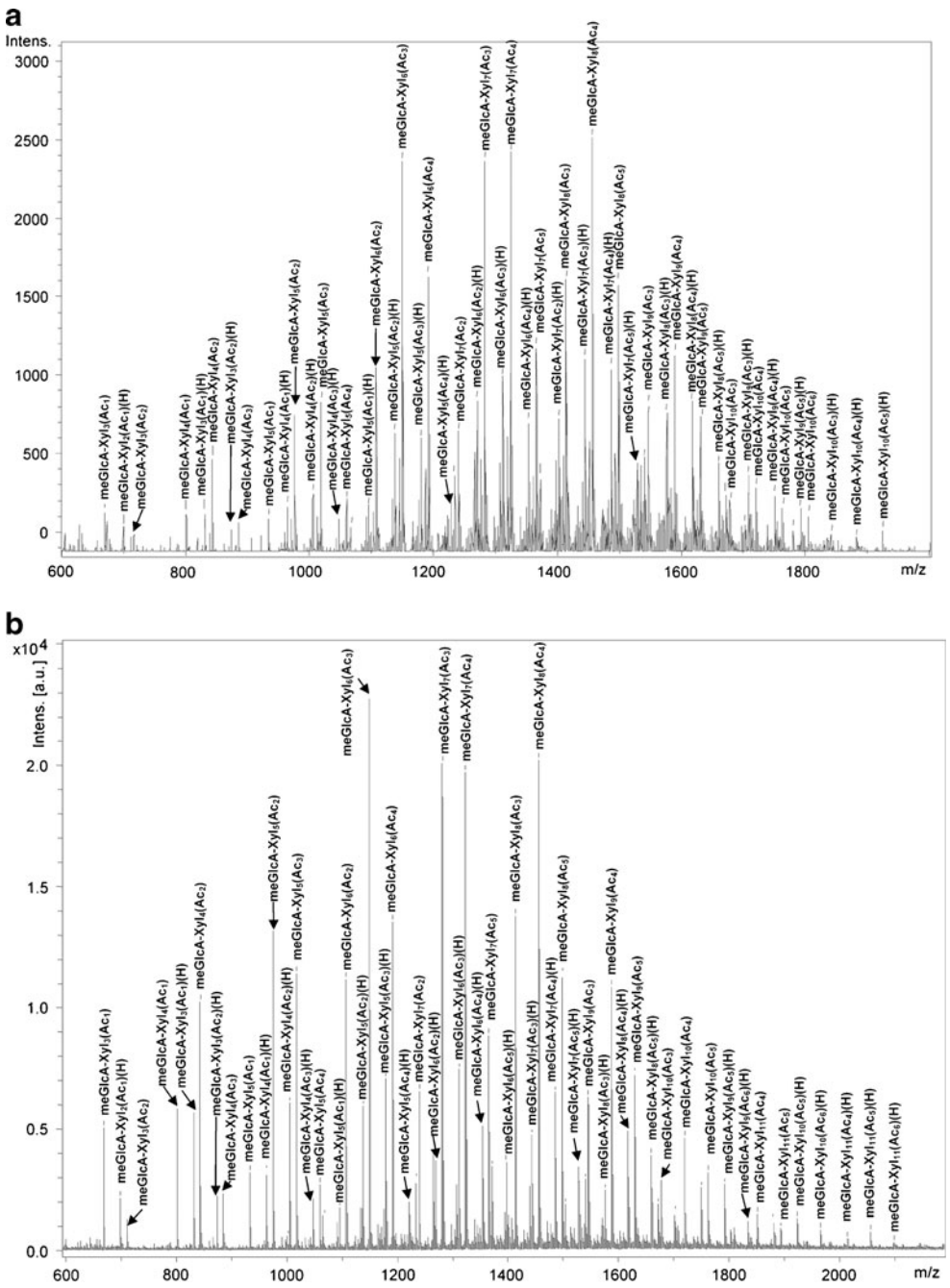

Fig. 2 A mass spectrum showing ion peaks (sodium adduct) representing acidic oligosaccharides purified from *Eucalyptus globulus* wood hydrolysate measured by (**a**) AP-MALDI-ITMS and (**b**) MALDI-TOF/MS

varying number of acetyl groups (Fig. 2 and Electronic Supplementary Material Table S2a). The detected acidic XOS ranged from 3 to 11 xylopyranosyl residues, with acetyl substitution from one to six residues. In addition, a series of acetylated meGlcA-XOS peaks carrying one hexose residue was also observed (Fig. 2 and Electronic Supplementary Material Table S2b). The hexose residue detected in the acidic oligosaccharides series was likely a galactopyranosyl or glucopyranosyl residue attached at the O-2 position of the meGlcA unit, as has been reported for *E. globulus* xylan by Evtuguin et al. [6]. The main peaks observed from both mass spectra were meGlcA-$Xyl_6(Ac_3)$, meGlcA-$Xyl_7(Ac_3)$, meGlcA-$Xyl_7(Ac_4)$ and meGlcA-$Xyl_8(Ac_4)$; however, the relative abundance of all four ion peaks were slightly different when the mass spectra from the two instruments were compared (Fig. 2). Most of the ion peaks were detectable by both systems, though the MALDI-TOF/MS system showed higher sensitivity for the detection of higher mass ion peaks similarly as with the neutral oligosaccharides. Minor peaks at *m/z*1,851, 1,893, 1,965, 2,013, 2,055 and 2,097, representing meGlcA-$Xyl_{11}(Ac_4)$, meGlcA-$Xyl_{11}(Ac_5)$, meGlcA-$Xyl_{10}(Ac_6)(H)$, meGlcA-$Xyl_{11}(Ac_4)(H)$, meGlcA-$Xyl_{11}(Ac_5)(H)$ and meGlcA-$Xyl_{11}(Ac_6)(H)$, respectively, were detected only

with the MALDI-TOF/MS (Fig. 2 and Electronic Supplementary Material Table S2).

Both neutral and acidic XOS profiles were successfully obtained from the AP-MALDI-ITMS measurements by using DHB as the matrix. Though the sensitivity of measurement of the AP-MALDI-ITMS system was poorer at higher masses due to the mass range limitation of up to *m/z*2,000 in the ultra scan mode, this system is likely more suitable for detecting neutral XOS with a higher degree of acetylation, as the ionization of analytes was softer at atmospheric condition, and therefore, the acetyl residues were more stable at the oligosaccharide moieties. The mass range of the ITMS can be extended to *m/z*4,000, but the mass accuracy will be concomitantly sacrificed up to ±1 Da [31]; thus, the reliable identification of ion peaks can be difficult. Therefore, the measurement of XOS samples of up to *m/z*4,000 was not attempted in this study.

AP-MALDI-ITMS analysis of the endoxylanase released XOS from hardwood

As the commonly used xylan isolation methods such as aqueous hydrothermal or alkaline extraction result changes in XOS structures, specific endo-1,4-β-D-xylanase hydrolysis was employed to release acetylated XOS directly from wood AIR sample. The GH10 endo-1,4-β-D-xylanase of *A. aculeatus* was selected since enzymes in this family are known to hydrolyse the xylan backbone close to the side groups, thus leaving them primarily at the non-reducing end of XOS [44–46]. The GH10 endo-1,4-β-D-xylanase applied was as a consequence able to produce shorter and fewer XOS than those produced by GH11 endo-1,4-β-D-xylanases [44], which simplified the interpretation of mass spectrum.

The mass spectra obtained from GH10 endo-1,4-β-D-xylanase hydrolysis of the aspen AIR sample are shown in Fig. 3. The hydrolysis resulted in the production of a vast array of different acetylated XOS. In the neutral fraction, mostly acetylated XOS (sodium adducts), with chain lengths from two to five xylopyranosyl residues, were detected (Fig. 3a and Electronic Supplementary Material Table S3a). Xylobiose (Xyl_2) carrying one acetyl group was the most abundant peak found in the mass spectrum, followed by Xyl_2 with two acetyl groups. The next abundant peaks were of xylotriose (Xyl_3) with two or three acetyl groups. Some minor peaks, representing xylotetraose (Xyl_4) and xylopentaose (Xyl_5) carrying three to five acetyl groups, were also detected and, in addition, minor peaks corresponding to non-acetylated Xyl_2 and Xyl_3 were found. Based on the result obtained, the GH10 endo-1,4-β-D-xylanase of *A. aculeatus* is producing mono- and di-acetylated xylobioses, presumably carrying the acetyl substitution at the non-reducing end xylopyranosyl residue, as the main neutral acetylated XOS.

Almost all acidic meGlcA-XOS liberated from aspen by *A. aculeatus* GH10 endo-1,4-β-D-xylanase were acetylated, and only very minor peaks of non-acetylated meGlcA-Xyl_3 were detected. The most abundant meGlcA-XOS contained three to seven xylopyranosyl residues with a single meGlcA residue and a varying number of acetyl groups (Fig. 3b and Electronic Supplementary Material Table S4b). The three main peaks observed from the mass spectrum were meGlcA-$Xyl_4(Ac_2)$, meGlcA-$Xyl_5(Ac_4)$ and meGlcA-$Xyl_6(Ac_5)$. Thus, the acetylation is limiting the action of *A. aculeatus* endo-1,4-β-D-xylanase as the hydrolysis of deacetylated GX by GH10 enzymes results in meGlcA-Xyl_3 as the major acidic XOS produced [44]. Later, it was also verified in this work that meGlcA-Xyl_3 was the main acidic XOS produced after the hydrolysis of deacetylated hybrid aspen AIR by *A. aculeatus* GH10 endo-1,4-β-D-xylanase (Fig. 9a).

The neutral and acidic XOS profiles resulting from the GH10 endo-1,4-β-D-xylanase hydrolysis of wood powder were different from those of the hydrothermally extracted *E. globulus* wood XOS (Fig. 1a, b and Electronic Supplementary Material Table S1 and S2). Longer XOS carrying lower amount of acetyl residues were not observed from the endo-1,4-β-D-xylanase hydrolysed aspen AIR sample, as these XOS were further degraded to shorter ones by the enzyme. The direct treatment of the AIR sample with endo-1,4-β-D-xylanase was able to liberate appreciable amounts of XOS for MS detection. This is the first report to show the feasibility of treating mature hardwood sample directly with a specific enzyme for the structural analysis of cell-wall polysaccharides. Though the degree of hydrolysis with a pure enzyme is limited due to the hindrance of other cell wall components, such as cellulose and lignin, the characterization of XOS from the enzyme-accessible part of xylan in the secondary plant cell wall is able to give useful information on the GX structural details.

The acidic XOS for glucuronoxylan structural comparison in different hardwood species

The AIR samples of aspen, birch and eucalyptus were directly hydrolysed by the *A. aculeatus* GH10 endo-1,4-β-D-xylanase, followed by AP-MALDI-ITMS analysis to evaluate GX structural differences between these hardwood species. The neutral XOS profiles were quite similar for all three species (data not shown), but the acidic XOS profile showed some differences among the three species. For sample comparison, the percentage peak intensities of the identified meGlcA-XOS from the mass spectra were calculated and shown in Fig. 4. The observed chain lengths of acetylated meGlcA-XOS in the aspen were from three to seven xylopyranosyl residues, whereas for birch and

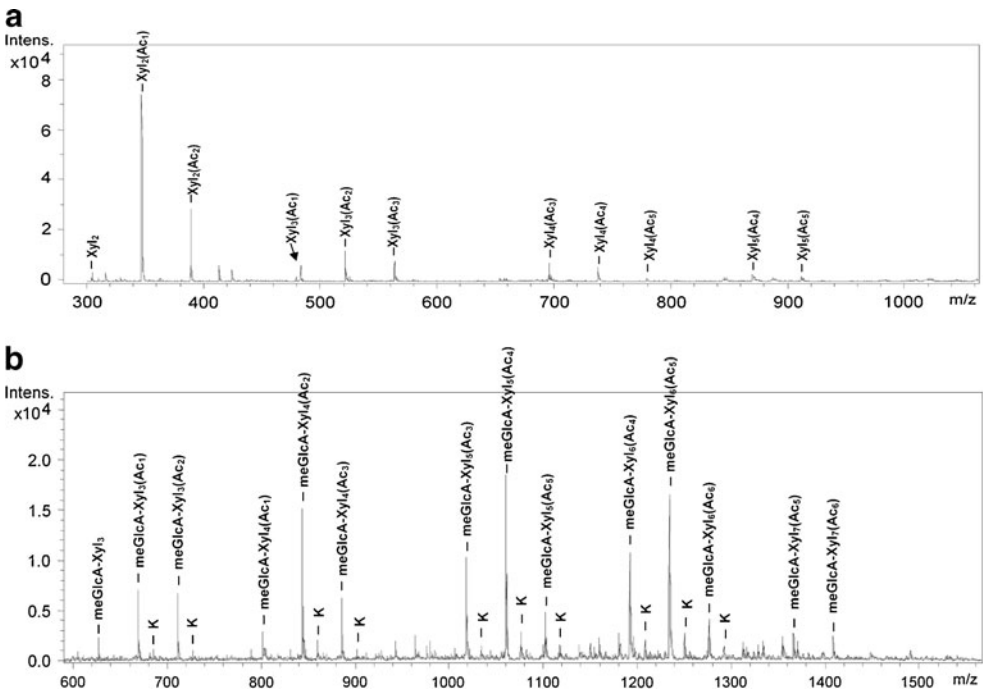

Fig. 3 AP-MALDI-ITMS mass spectra showing (**a**) neutral and (**b**) acidic XOS liberated from aspen AIR by GH10 endo-1,4-β-D-xylanase hydrolysis. Potassium adduct peaks were also identified and labelled with K

eucalyptus hydrolysates, the oligosaccharides were somewhat shorter, from three to six xylopyranosyl residues. The peaks representing highly acetylated acidic XOS, such as meGlcA-$Xyl_5(Ac_6)$ and meGlcA-$Xyl_6(Ac_6)$, were only observed in the aspen-derived sample. In contrast to the three main peaks observed in the aspen sample, the most abundant peak observed in the birch and eucalyptus samples was meGlcA-$Xyl_4(Ac_2)$. In addition to the series of meGlcA-XOS observed from all three hardwood species, several peaks representing meGlcA-XOS carrying a hexose residue were observed from the analysis of acidic XOS in the eucalyptus sample (Fig. 5). Similar acidic XOS were also detected earlier in the XOS sample from hydrothermally treated *E. globulus* wood (Electronic Supplementary Material Table S2 and Fig. 2).

The overall meGlcA-XOS fragments derived from birch and eucalyptus AIR samples after GH10 endo-1,4-β-D-xylanase hydrolysis were shorter than those derived from the aspen AIR sample, indicating that the degree of substitution, which restricts the action of endo-1,4-β-D-xylanase, was lower in birch and eucalyptus than in aspen. This observation was supported by a lower amount of acetyl found in birch and eucalyptus (Table 1). The average meGlcA substitution of Xyl residues in aspen, birch and eucalyptus were 1:11, 1:17 and 1:7, respectively, whereas the average degree of acetylation per Xyl residue was 0.84, 0.72 and 0.74, respectively. A small part of acetylation in hardwood can also be in polymers other than GX, but this was not taken into account in the calculation. The meGlcA substitution level in eucalyptus seems to be the highest; however, this result was not implied by the higher hindrance effect on the enzymatic action as longer XOS fragments were seen in aspen hydrolysate. Clearly, as the overall acetyl substitution per Xyl residue was significantly higher than that of the meGlcA residues, the acetyl substitution in hardwood GX was much more restrictive to enzyme hydrolysis, and thus, the distribution of the chain lengths of the XOS obtained reflect mainly the differences in acetylation. Indeed, the lengths of the acetylated XOS liberated in the endo-1,4-β-D-xylanase hydrolysis of the three studied hardwood species correlated well with the analysed acetylation, which was highest in the aspen wood, and thus resulted in the longest acetylated XOS. However, it must be realized that the enzyme hydrolysis is also affected by the distribution of substituents along the xylan backbone and not only by the degree of substitution. The previously reported degrees of acetylation per Xyl residue of purified aspen, birch and eucalyptus GX were 0.6, 0.4 and 0.6, respectively [3, 6, 47]. However, these GX were isolated by different methods, and thus, the values are not directly comparable. Moreover, these GX were isolated under more severe conditions than XOS in this work; thus, partial deacetylation during isolation process cannot be excluded.

Endoxylanase released XOS from *A. thaliana* AIR sample

The neutral XOS fraction from the *A. thaliana*, detected by AP-MALDI-ITMS, possessed almost a similar profile as those obtained from aspen, except that a series of minor hexose peaks were also detected, which most probably originated from starch due to the amylase treatment applied

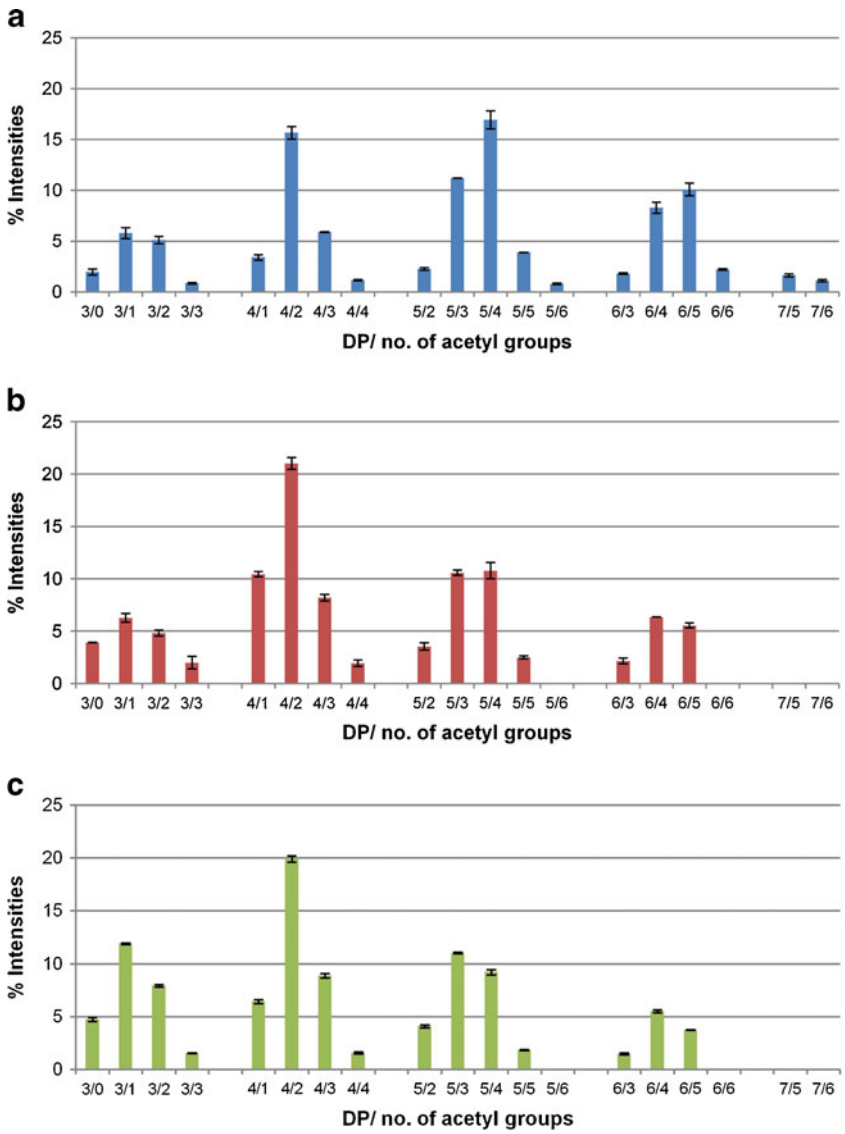

Fig. 4 Graphs showing percentage peak intensities of meGlcA-XOS identified from the AP-MALDI-ITMS mass spectra. The meGlcA-XOS were liberated from (**a**) aspen, (**b**) birch and (**c**) eucalyptus AIR samples by GH10 endo-1,4-β-D-xylanase hydrolysis. The *error bars* represent standard deviation of duplicate samples. DP = degree of polymerization

in the sample preparation (Fig. 6a and Electronic Supplementary Material Table S4a). Analysis of acidic XOS revealed the presence of two series of acidic XOS corresponding to acetylated meGlcA-XOS (Fig. 6b and Electronic Supplementary Material Table S4b) and GlcA-XOS (Fig. 6b and Electronic Supplementary Material Table S4c), respectively. The chain lengths for the GlcA-XOS series were from three to six xylopyranosyl residues,

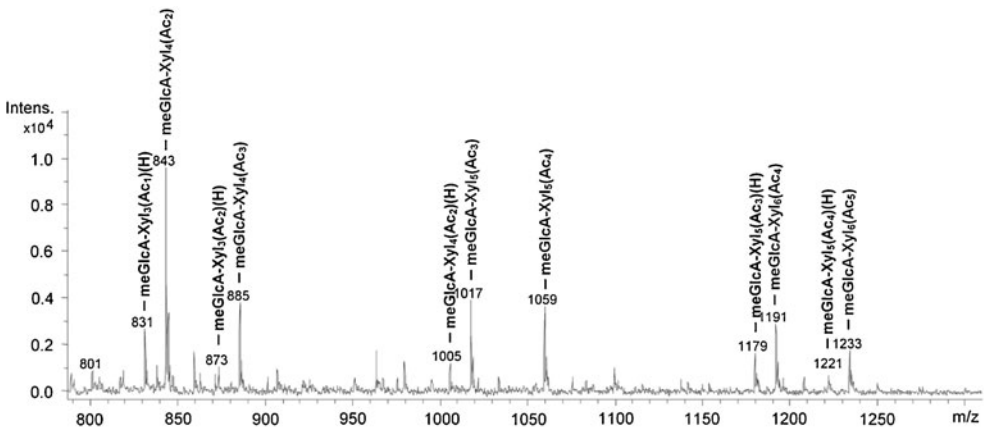

Fig. 5 Mass spectrum showing meGlcA-XOS carrying one hexose residue identified from the analysis of acidic XOS derived from the eucalyptus endoxylanase hydrolysate by AP-MALDI-ITMS in the positive ion mode

Table 1 The amount of xylopyranosyl (Xyl), 4-*O*-methylglucopyranosyl uronic acid (meGlcA), and acetyl residues that are present in aspen, birch and eucalyptus wood powders

	Monosaccharides and acetyl content (μmol/100 mg wood powder)			Average molar ratio	
	Xyl	meGlcA	Acetyl (Ac)	meGlcA:Xyl	Ac:Xyl
Aspen	130±13	12±2.1	109±10	1:11	0.84
Birch	180±13	11±0.9	129±14	1:17	0.72
Eucalyptus	112±3	17±0.6	83±7	1:7	0.74

The values were calculated as mean of triplicate samples

while for the meGlcA-XOS series, the chain lengths detected were from three to seven xylopyranosyl residues.

The meGlcA-XOS peak intensities were in most cases higher than those of the adjacent GlcA-XOS peaks, indicating that there is more meGlcA in the GX of *A. thaliana* than GlcA. However, the intensities of the two peaks, representing GlcA-$X_4(Ac_1)$ and GlcA-$X_5(Ac_2)$, were found higher than those of adjacent meGlcA-XOS peaks representing meGlcA-$Xyl_4(Ac_1)$ and meGlcA-$Xyl_5(Ac_2)$, respectively. Interestingly, these acidic XOS contained least acetyl residues in each corresponding chain length series. This may indicate that the region close to the GlcA in the GX of *A. thaliana* is somewhat less acetylated. It is suggested that the methylation of GlcA in GX of *A. thaliana* occurs after the GlcA residues are attached to the xylan backbone [44]. The acetylation of GX can also take place at the latter stage of xylan biosynthesis, together with methylation either simultaneously or sequentially; thus, part of the xylan chains in the cell wall carrying non-methylated GlcA are less acetylated. However, this hypothesis is still subject for further analysis. To our knowledge, no previous reports are published on the acetylation of GX in *A. thaliana*, which is presently the most important plant model for GX biosynthesis studies [7–9]. To date, the GX present in the wild type and mutant plants has been isolated by alkaline extraction prior to characterization, and therefore, the acetylation of GX in *A. thaliana* was not revealed.

MS^n analysis of the isomeric aldotetrauronic acids

The AP-MALDI ion source, operating at ambient pressure, can be conveniently linked to the ITMS and therefore has the advantage over MALDI-TOF/MS to perform multi-stages mass fragmentation for structural elucidation. For structural

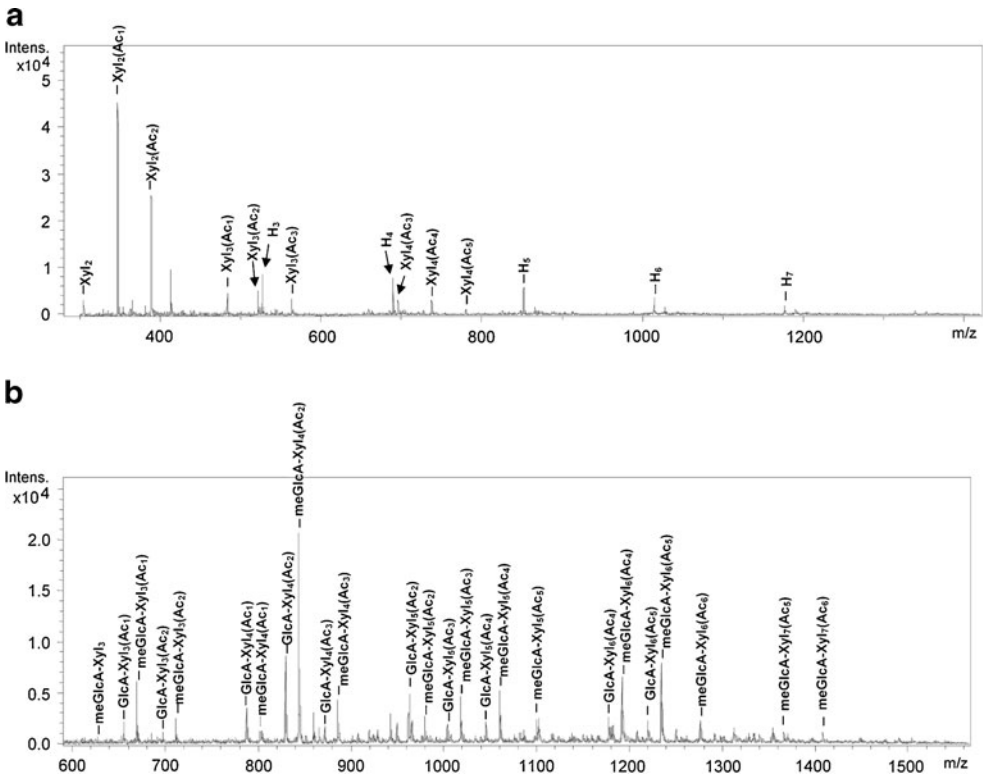

Fig. 6 AP-MALDI-ITMS mass spectra showing (**a**) neutral and (**b**) acidic XOS liberated by GH10 endo-1,4-β-D-xylanase hydrolysis from *Arabidopsis thaliana* AIR of inflorescence stems

analysis, the MALDI-TOF/MS needs an additional TOF system. The feasibility of AP-MALDI-ITMS to determine the accurate position of substituents in XOS was tested by MS^n analysis with two isomeric aldotetrauronic acid samples: UXX and XUX. These XOS were prepared from alkaline extracted birch GX, and their structures were determined by NMR spectroscopy (Koutaniemi et al., in preparation). The UXX was an aldotetrauronic acid containing a meGlcA residue α-(1→2) linked to the non-reducing end of Xyl_3, whereas the XUX contained a meGlcA residue α-(1→2) linked to the internal xylopyranosyl residue in Xyl_3.

The MS^2 spectrum of $[UXX+Na]^+$ (*m/z*627) is shown in Fig. 7a. The main peak observed was at *m/z*437, indicating the loss of 190 Da from the precursor ion, followed by the product ion at *m/z*305, indicating the loss of 132 Da. These product ions show that the cleavage of meGlcA from the Xyl_3 backbone was the predominant fragmentation pathway followed by the loss of one xylopyranosyl residue. The ESI-MS/MS analysis of meGlcA-$Xyl_{5–8}$ was previously demonstrated, and the main product observed was the XOS core backbone that resulted from the loss of meGlcA residue [48]. Less intensive ion peaks at *m/z*477 and *m/z* 345 indicated the cleavages of glycosidic bonds and therefore suggesting that the meGlcA was located at the terminal end of Xyl_3 backbone. Since the NMR spectroscopic analysis confirmed the position of the meGlcA at the non-reducing end, we can deduce that these two peaks were representing B_3 and B_2 ions, respectively (Fig. 7a). The product ions were named according to the nomenclature introduced by Domon and Costello [49]. The ion peak *m/z* 479 can be attributed by proton migration from the adjacent xylopyranoyl residue to the B_3 ion (*m/z*477). In the fragmentation pathway proposed by Domon and Costello, employing a FAB-MS/MS analysis in the positive ion mode, the cleavage of glycosidic bond was often accompanied by proton transfer. No C/Z ions were observed in the MS^2 spectrum. Most of the reports describing MS^n analysis of oligosaccharides using ESI or AP-MALDI techniques propose that the cross ring cleavage was taking place at the reducing end of the oligosaccharides [31, 34, 48]. Therefore, the product ion at *m/z*567 observed from the MS^2 of UXX was likely due to the loss of $C_2H_4(OH)_2$ at the reducing end and therefore named as $^{0,2}A_3$. However, cross ring cleavage at the non-reducing end cannot be precluded in this case since we did not derivatise the reducing end to confirm the position.

The MS^2 spectrum of $[XUX+Na]^+$ (*m/z*627) is shown in Fig. 7b. In contrast to the MS^2 spectrum of UXX, the main peak observed from the MS^2 analysis of XUX was $^{0,2}A_3$ (*m/z* 567). This result suggests that cross ring cleavage (loss of 60 Da) was the main fragmentation pathway. The ion peak representing the loss of meGlcA residue (*m/z*437), $Y_{2\alpha}$, was identified as the second most abundant peak. Less intensive peaks indicating glycosidic bond cleavages were also observed; however, because the meGlcA residue was residing at the middle position of the Xyl_3 backbone, these product ions can be denoted as B/Y ions or C/Z ions. Therefore, the product ions at *m/z*495 and 477 can be denoted as C_2/Y_2 and B_2/Z_2 ions, respectively. The MS^2 analysis of both isomeric aldotetrauronic acids, UXX and XUX, clearly showed that the fragmentation pathways were different due to the residing position of the meGlcA residue along the Xyl_3 backbone.

The ion peaks resulting from the cleavage of the first glycosidic bond from the reducing end of Xyl_3 was *m/z*477 for UXX and XUX, respectively; thus, this ion was chosen for MS^3 analysis for further structural elucidation. The MS^3

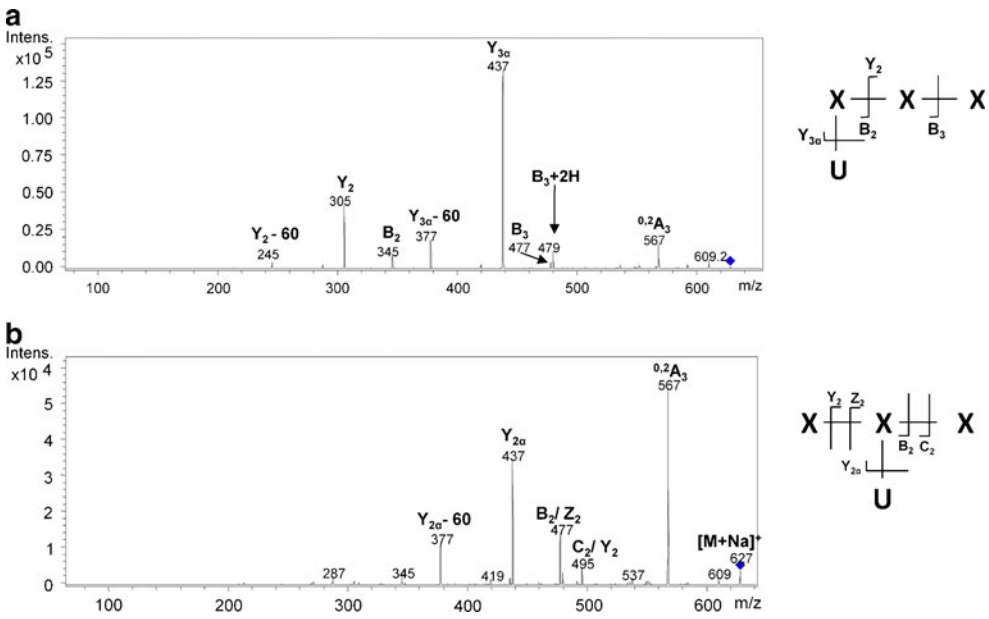

Fig. 7 MS^2 spectra of *m/z*627 measured by AP-MALDI-ITMS with their possible product ions and nomenclature derived from aldotetrauronic acid: (**a**) UXX and (**b**) XUX

analysis of *m/z*477 derived from UXX and XUX were shown in Fig. 8a and b, respectively. The mass spectra derived from both structures were quite similar as the main peak observed was *m/z*345, representing glycosidic bond cleavage between two adjacent xylopyranosyl residues. This ion peak was denoted as B_1 and Y_1 ion from the MS^3 of UXX and XUX, respectively. In addition, the cleavage between the meGlcA residues with Xyl_2 in both structures was identified by ion peak *m/z*287. The identification of the meGlcA location in both structures was differentiated by the minor peaks observed. The characteristic peak identified from the MS^3 of UXX was *m/z*363 ($^*C_1$ ion) and confirmed that the meGlcA residue was residing at the non-reducing end of Xyl_2, whereas minor peak *m/z*155 ($^*B_1$ ion) observed from the MS^3 of XUX confirmed that the meGlcA residue was residing at the internal xylopyranosyl residue. In addition, the meGlcA fragment was only observed from the MS^3 of XUX and identified as *m/z*213 ($B_{2\alpha}$ ion).

MS^n analysis of the acidic XOS derived from GH10 endoxylanase hydrolysis of deacetylated AIR of hybrid aspen

The GH10 endo-1,4-β-D-xylanase was also applied on deacetylated young hybrid aspen AIR to compare the XOS profile as obtained from the acetylated GX. The acetylated neutral and acidic XOS profiles derived from the GH10 endo-1,4-β-D-xylanase hydrolysed young hybrid aspen were close to the aspen mass spectra shown earlier in this work (Fig. 3a, b). The AP-MALDI-ITMS mass spectrum showing ion peaks of acidic XOS derived from the deacetylated young poplar AIR is presented in Fig. 9a. The main peak observed was at *m/z*627, representing Xyl_3 carrying one meGlcA residue most probably residing at the non-reducing end [44]. Minor peak at *m/z*669 representing mono-acetylated meGlcA-Xyl_3 was also present in the XOS sample, showing that this sample was not fully deacetylated. In addition, there was a minor ion peak at *m/z*613, which can be attributed by the non-methylated glucuronic acid. Due to the advantage of AP-MALDI-ITMS to perform tandem MS, both peaks at *m/z*627 and 613 were selected for MS^2 analysis to confirm their structures and the position of the uronic acid residue (Fig. 9b, c). Both compounds showed similar product ions and glycosidic bond cleavages as described in the MS^2 analysis of UXX (Fig. 7a), except that the masses for B_2 and B_3 ions in the MS^2 analysis of *m/z*613 were 14 Da smaller, suggesting that the non-methylated glucuronic acid was present in this oligosaccharide. The observation of product ions at *m/z*213 and 199 confirmed the presence of meGlcA and GlcA, respectively, when the B_2 ions from both compounds were subjected to MS^3 analysis (Fig. 9b, c). The ion peak intensity at *m/z*613 was only 4.3%, relative to the main peak at *m/z*627, indicating that the amount of GlcA present in the GX of poplar is very low. Indeed, the GlcA was hardly observed from the GC chromatograms obtained from the analysis of acid methanolysed hardwood powder (data not shown). Thus, the identification of low amount of the non-methylated glucuronic acid by conventional analysis is difficult, but in the present study, AP-MALDI-ITMS was shown to be sensitive enough, also in MS^3 measurements, for reliable identification of minor component present in the endo-1,4-β-D-xylanase released XOS sample. However,

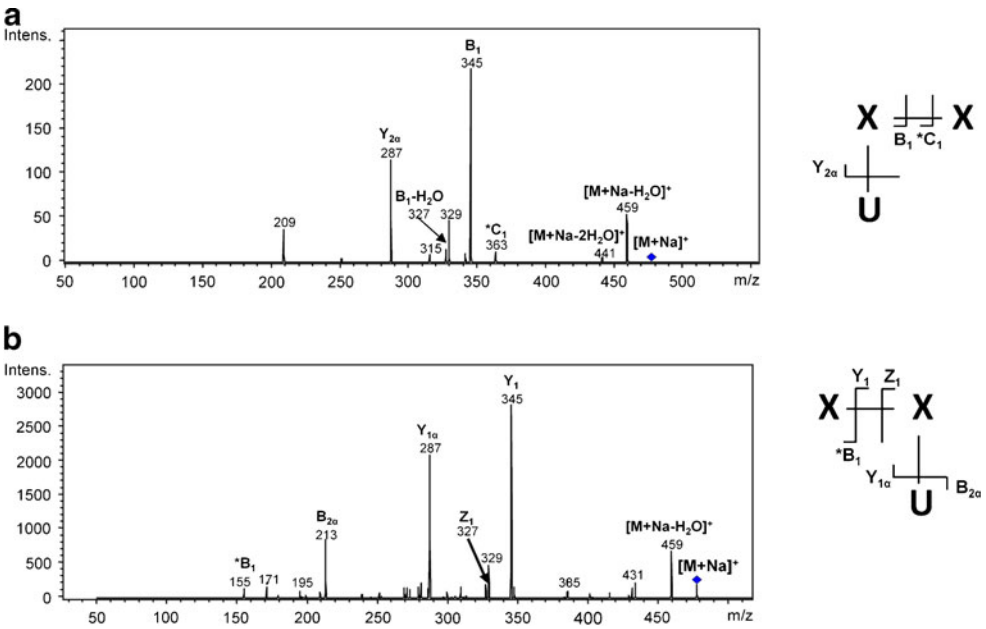

Fig. 8 MS^3 spectra of *m/z*477 measured by AP-MALDI-ITMS with their possible product ions and nomenclature of the precursor ion derived from aldotetrauronic acid: (**a**) UXX and (**b**) XUX

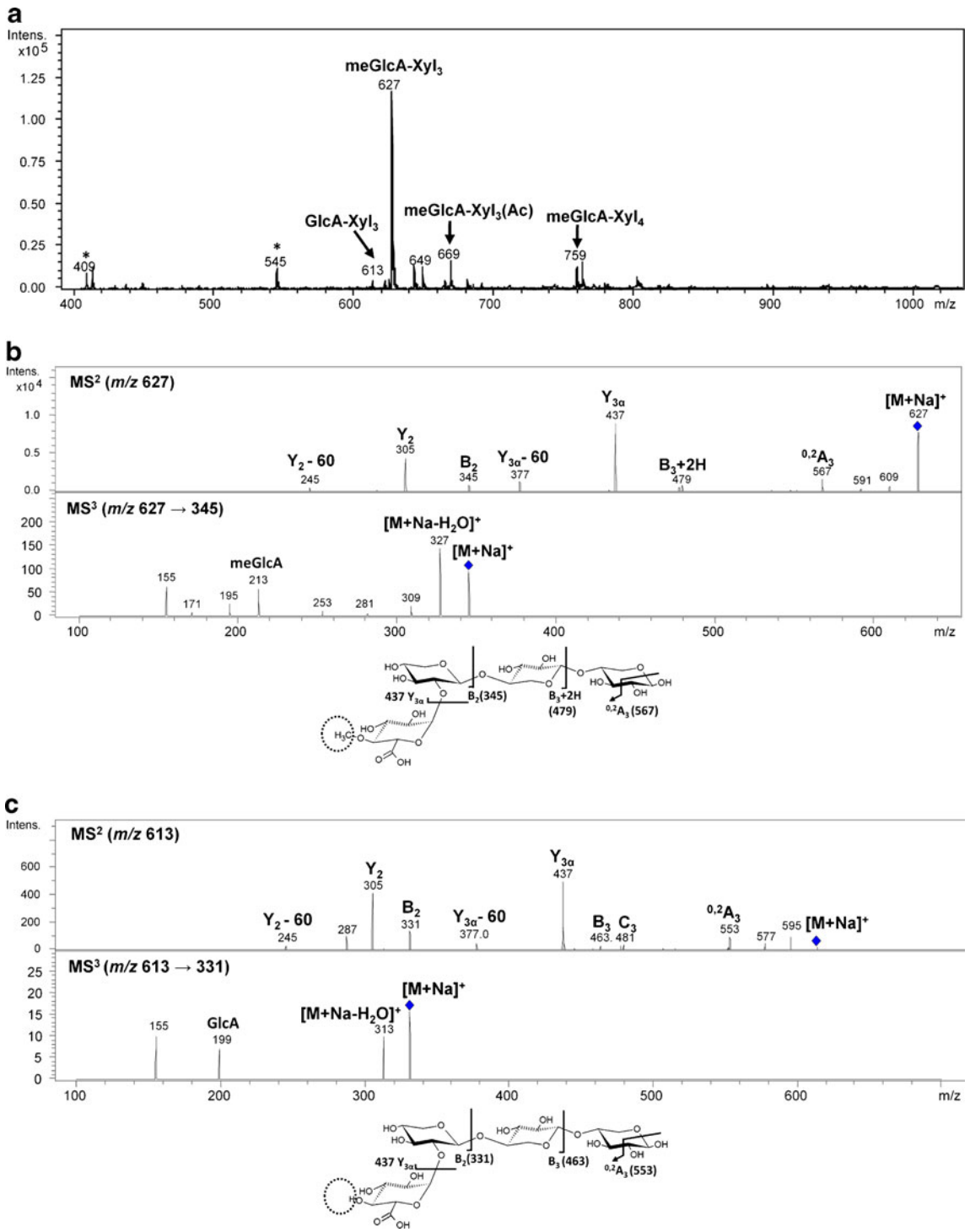

Fig. 9 (**a**) An AP-MALDI-ITMS mass spectrum showing a mixture of acidic XOS derived from GH10 endo-1,4-β-D-xylanase hydrolysis of deacetylated young hybrid aspen AIR. MS^2 and MS^3 analysis of (**b**) the main peak at *m/z*627 and *m/z*627→345 and (**c**) a minor peak at *m/z*613 and *m/z*613→331 measured by AP-MALDI-ITMS. The peaks labelled with *asterisks* were originated from matrix clusters

deacetylation of the wood sample was a prerequisite step prior to enzyme hydrolysis to limit the number of XOS produced, which enabled the detection of the minor substituents in GX.

Conclusions

AP-MALDI-ITMS was shown to be a potential tool to analyse plant cell wall-derived oligosaccharides, in addition

to commonly used MALDI-TOF/MS. The AP-MALDI-ITMS better detected the neutral XOS with higher degree of acetylation than the MALDI-TOF/MS did; this was despite the fact that the sensitivity of measurement at higher mass range was poorer in AP-MALDI-ITMS than in the MALDI-TOF/MS. In addition, AP-MALDI-ITMS produced results that corresponded better to the actual compositions of the XOS sample that contained a low amount of HOS as impurity. The endo-1,4-β-D-xylanase applied was shown to be able to liberate enough XOS for MS characterization, even from the mature hardwood stem sample without any tedious pre-treatment such as delignification. In addition to hardwood samples, acetylated XOS were also detected for the first time in the endo-1,4-β-D-xylanase hydrolysate derived from *A. thaliana* sample. The AP-MALDI-ITMS was shown to be sensitive enough for MS^n analysis for the structural analysis of acidic XOS, and for the minor components such as GlcA containing XOS present in the hydrolysate of deacetylated young hybrid aspen. The combination of selective endo-1,4-β-D-xylanase hydrolysis with the sensitive AP-MALDI-ITMS analysis will be an invaluable method for structural comparison of native or in vivo modified GX. In the future, statistical methods such as the principle component analysis (PCA) could be applied for the improved comparison of the samples.

Acknowledgements We thank Dr. Nisse Kalkkinen and Gunilla Rönnholm (Protein Chemistry Research Group, Institute of Biotechnology, Helsinki) for the help in MALDI-TOF/MS analysis. We thank Prof. Juan Carlos Parajó of University of Vigo, Spain for the XOS sample isolated from hydrothermally treated *E. globulus* wood and Prof. Stefan Willför of Åbo Akademi University, Finland for the aspen, birch and eucalyptus wood powders. The financial support from the Academy of Finland and Formas through the WoodWisdom-Net Programme (HemiPop project no. 1124281) and Glycoscience Graduate School (S.-L.C) are gratefully acknowledged.

References

1. Aspinall GO (1980) Chemistry of cell wall polysaccharides. Biochem Plants 3:473–500
2. Timell TE (1967) Recent progress in the chemistry of wood hemicelluloses. Wood Sci Technol 1:45–70
3. Teleman A, Lundqvist J, Tjerneld F, Stålbrand H, Dahlman O (2000) Characterization of acetylated 4-*O*-methylglucuronoxylan isolated from aspen employing 1H and 13C NMR spectroscopy. Carbohydr Res 329:807–815
4. Naran R, Black S, Decker SR, Azadi P (2009) Extraction and characterization of native heteroxylans from delignified corn stover and aspen. Cellulose 16:661–675
5. Goncalves VMF, Evtuguin DV, Domingues MRM (2008) Structural characterization of the acetylated heteroxylan from the natural hybrid *Paulownia elongata*/*Paulownia fortunei*. Carbohydr Res 343:256–266
6. Evtuguin DV, Tomas JL, Silva AMS, Neto CP (2003) Characterization of an acetylated heteroxylan from *Eucalyptus globulus* Labill. Carbohydr Res 338:597–604
7. Brown DM, Goubet F, Wong VW, Goodacre R, Stephens E, Dupree P, Turner SR (2007) Comparison of five xylan synthesis mutants reveals new insight into the mechanisms of xylan synthesis. Plant J 52:1154–1168
8. Peña MJ, Zhong RQ, Zhou GK, Richardson EA, O'Neill MA, Darvill AG, York WS, Zheng HY (2007) *Arabidopsis irregular xylem8* and *irregular xylem9*: implications for the complexity of glucuronoxylan biosynthesis. Plant Cell 19:549–563
9. Wu AM, Rihouey C, Seveno M, Hörnblad E, Singh SK, Matsunaga T, Ishii T, Lerouge P, Marchant A (2009) The *Arabidopsis* IRX10 and IRX10-LIKE glycosyltransferases are critical for glucuronoxylan biosynthesis during secondary cell wall formation. Plant J 57:718–731
10. Sjöström E (1993) Wood chemistry: fundamentals and applications, 2nd edn. Academic, California
11. Lerouxel O, Choo TS, Seveno M, Usadel B, Faye L, Lerouge P, Pauly M (2002) Rapid structural phenotyping of plant cell wall mutants by enzymatic oligosaccharide fingerprinting. Plant Physiol 130:1754–1763
12. Westphal Y, Schols HA, Voragen AGJ, Gruppen H (2010) MALDI-TOF MS and CE-LIF fingerprinting of plant cell wall polysaccharide digests as a screening tool for *Arabidopsis* cell wall mutants. J Agric Food Chem 58:4644–4652
13. Jacobs A, Dahlman O (2001) Enhancement of the quality of MALDI mass spectra of highly acidic oligosaccharides by using a Nafion-coated probe. Anal Chem 73:405–410
14. Enebro J, Momcilovic D, Siika-aho M, Karlsson S (2009) Investigation of endoglucanase selectivity on carboxymethyl cellulose by mass spectrometric techniques. Cellulose 16:271–280
15. Jacobs A, Larsson PT, Dahlman O (2001) Distribution of uronic acids in xylans from various species of soft- and hardwood as determined by MALDI mass spectrometry. Biomacromolecules 2:979–990
16. Kabel MA, Schols HA, Voragen AGJ (2002) Complex xylo-oligosaccharides identified from hydrothermally treated *Eucalyptus* wood and brewery's spent grain. Carbohydr Polym 50:191–200
17. Teleman A, Nordstrom M, Tenkanen M, Jacobs A, Dahlman O (2003) Isolation and characterization of *O*-acetylated glucomannans from aspen and birch wood. Carbohydr Res 338:525–534
18. Teleman A, Lundqvist J, Tjerneld F, Stålbrand H, Dahlman O (2002) Characterization of water-soluble hemicelluloses from spruce and aspen employing SEC/MALDI mass spectroscopy. Carbohydr Res 337:711–717
19. Korner R, Limberg G, Mikkelsen JD, Roepstorff P (1998) Characterization of enzymatic pectin digests by matrix-assisted laser desorption/ionization mass spectrometry. J Mass Spectrom 33:836–842
20. Zaia J (2004) Mass spectrometry of oligosaccharides. Mass Spectrom Rev 23:161–227
21. Powell AK, Harvey DJ (1996) Stabilization of sialic acids in N-linked oligosaccharides and gangliosides for analysis by positive ion matrix-assisted laser desorption/ionization mass spectrometry. Rapid Commun Mass Spectrom 10:1027–1032
22. Bagag A, Laprevote O, Hirsch J, Kovacik V (2008) Atmospheric pressure photoionization mass spectrometry of per-*O*-methylated oligosaccharides related to D-xylans. Carbohydr Res 343:2813–2818
23. Fernandez LEM, Obel N, Scheller HV, Roepstorff P (2003) Characterization of plant oligosaccharides by matrix-assisted laser desorption/ionization and electrospray mass spectrometry. J Mass Spectrom 38:427–437
24. Matamoros Fernandez LE, Obel N, Scheller HV, Roepstorff P (2004) Differentiation of isomeric oligosaccharide structures by ESI tandem MS and GC-MS. Carbohydr Res 339:655–664

25. Reis A, Pinto P, Evtuguin DV, Neto CP, Domingues P, Ferrer-Correia AJ, Domingues MRM (2005) Electrospray tandem mass spectrometry of underivatised acetylated xylo-oligosaccharides. Rapid Commun Mass Spectrom 19:3589–3599
26. Reis A, Pinto P, Coimbra MA, Evtuguin DV, Neto CP, Ferrer Correia AJ, Domingues MRM (2004) Structural differentiation of uronosyl substitution patterns in acidic heteroxylans by electrospray tandem mass spectrometry. J Am Soc Mass Spectrom 15:43–47
27. Quemener B, Ordaz-Ortiz JJ, Saulnier L (2006) Structural characterization of underivatized arabino-xylo-oligosaccharides by negative-ion electrospray mass spectrometry. Carbohydr Res 341:1834–1847
28. Reinhold VN, Reinhold BB, Costello CE (1995) Carbohydrate molecular weight profiling, sequence, linkage, and branching data: ES-MS and CID. Anal Chem 67:1772–1784
29. Harvey DJ (2006) Analysis of carbohydrates and glycoconjugates by matrix-assisted laser desorption/ionization mass spectrometry: an update covering the period 1999-2000. Mass Spectrom Rev 25:595–662
30. Laiko VV, Baldwin MA, Burlingame AL (2000) Atmospheric pressure matrix-assisted laser desorption/ionization mass spectrometry. Anal Chem 72:652–657
31. Creaser CS, Reynolds JC, Harvey DJ (2002) Structural analysis of oligosaccharides by atmospheric pressure matrix-assisted laser desorption/ionization quadrupole ion trap mass spectrometry. Rapid Commun Mass Spectrom 16:176–184
32. Zhang J, LaMotte L, Dodds ED, Lebrilla CB (2005) Atmospheric pressure MALDI fourier transform aass spectrometry of labile oligosaccharides. Anal Chem 77:4429–4438
33. Moyer SC, Marzilli LA, Woods AS, Laiko VV, Doroshenko VM, Cotter RJ (2003) Atmospheric pressure matrix-assisted laser desorption/ionization (AP MALDI) on a quadrupole ion trap mass spectrometer. Int J Mass Spectrom 226:133–150
34. Tan PV, Taranenko NI, Laiko VV, Yakshin MA, Prasad CR, Doroshenko VM (2004) Mass spectrometry of N-linked oligosaccharides using atmospheric pressure infrared laser ionization from solution. J Mass Spectrom 39:913–921
35. Gullón P, González-Muñoz MJ, Domínguez H, Parajó JC (2008) Membrane processing of liquors from *Eucalyptus globulus* autohydrolysis. J Food Eng 87:257–265
36. Zablackis E, Huang J, Mueller B, Darvill AG, Albersheim P (1995) Characterization of the cell-wall polysaccharides of *Arabidopsis thaliana* leaves. Plant Physiol 107:1129–1138
37. Packer NH, Lawson MA, Jardine DR, Redmond JW (1998) A general approach to desalting oligosaccharides released from glycoproteins. Glycoconj J 15:737–747
38. Enebro J, Karlsson S (2006) Improved matrix-assisted laser desorption/ionization time-of-flight mass spectrometry of carboxymethyl cellulose. Rapid Commun Mass Spectrom 20:3693–3698
39. Salo PK, Salomies H, Harju K, Ketola RA, Kotiaho T, Yli-Kauhaluoma J, Kostiainen R (2005) Analysis of small molecules by ultra thin-layer chromatography-atmospheric pressure matrix-assisted laser desorption/ionization mass spectrometry. J Am Soc Mass Spectrom 16:906–915
40. Fauré R, Courtin CM, Delcour JA, Dumon C, Faulds CB, Fincher GB, Fort S, Fry SC, Halila S, Kabel MA, Pouvreau L, Quemener B, Rivet A, Saulnier L, Schols HA, Driguez H, O'Donohue MJ (2009) A brief and informationally rich naming system for oligosaccharide motifs of heteroxylans found in plant cell walls. Aust J Chem 62:533–537
41. Sundberg A, Sundberg K, Lillandt C, Holmbom B (1996) Determination of hemicelluloses and pectins in wood and pulp fibers by acid methanolysis and gas chromatography. Nord Pulp Pap Res J 11:216–226
42. Pastell H, Virkki L, Harju E, Tuomainen P, Tenkanen M (2009) Presence of 1→3-linked 2-*O*-β-D-xylopyranosyl-α-L-arabinofuranosyl side chains in cereal arabinoxylans. Carbohydr Res 344:2480–2488
43. Li YCL, Cheng S-W, Chan T-WD (1998) Evaluation of ammonium salts as co-matrixes for matrix-assisted laser desorption/ionization mass spectrometry of oligonucleotides. Rapid Commun Mass Spectrom 12:993–998
44. Biely P, Vršanská M, Tenkanen M, Kluepfel D (1997) Endo-β-1,4--xylanase families: differences in catalytic properties. J Biotechnol 57:151–166
45. Rantanen H, Virkki L, Tuomainen P, Kabel M, Schols H, Tenkanen M (2007) Preparation of arabinoxylobiose from rye xylan using family 10 *Aspergillus aculeatus* endo-1,4-β-D-xylanase. Carbohydr Polym 68:350–359
46. Pastell H, Tuomainen P, Virkki L, Tenkanen M (2008) Step-wise enzymatic preparation and structural characterization of singly and doubly substituted arabinoxylo-oligosaccharides with non-reducing end terminal branches. Carbohydr Res 343:3049–3057
47. Teleman A, Tenkanen M, Jacobs A, Dahlman O (2002) Characterization of *O*-acetyl-(4-*O*-methylglucurono)xylan isolated from birch and beech. Carbohydr Res 337:373–377
48. Reis A, Domingues MRM, Domingues P, Ferrer-Correia AJ, Coimbra MA (2003) Positive and negative electrospray ionization tandem mass spectrometry as a tool for structural characterization of acid released oligosaccharides from olive pulp glucuronoxylans. Carbohydr Res 338:1497–1505
49. Domon B, Costello CE (1988) A systematic nomenclature for carbohydrate fragmentations in FAB-MS/MS spectra of glycoconjugates. Glycoconj J 5:397–409